Synthetic, Structural, Spectroscopic and Solution Speciation Studies of the Binary Al(III)–Quinic Acid System. Relevance of soluble Al(III)–hydroxycarboxylate species to molecular…

ARTICLE *in* POLYHEDRON · SEPTEMBER 2008

Impact Factor: 2.01 · DOI: 10.1016/j.poly.2008,06.029

9 AUTHORS, INCLUDING:

Melita Menelaou
Tohoku University
36 PUBLICATIONS **161** CITATIONS
SEE PROFILE

Andrea Lakatos
Goethe-Universität Frankfurt am Main
34 PUBLICATIONS **674** CITATIONS
SEE PROFILE

Constantin Mateescu
Banat University of Agronomical Sciences a…
37 PUBLICATIONS **97** CITATIONS
SEE PROFILE

Panagiotis Zoumpoulakis
National Hellenic Research Foundation
66 PUBLICATIONS **735** CITATIONS
SEE PROFILE

Polyhedron 27 (2008) 2911–2920

Contents lists available at ScienceDirect

Polyhedron

journal homepage: www.elsevier.com/locate/poly

Synthetic, structural, spectroscopic and solution speciation studies of the binary Al(III)–quinic acid system. Relevance of soluble Al(III)–hydroxycarboxylate species to molecular toxicity

Catherine Gabriel [a], Melita Menelaou [a], Markos Daskalakis [b], Andrea Lakatos [c], Tamas Kiss [c,*], Constantin Mateescu [d], Raphael G. Raptis [e], Panagiotis Zoumpoulakis [f], Athanasios Salifoglou [a,*]

[a] Department of Chemical Engineering, Laboratory of Inorganic Chemistry, Aristotle University of Thessaloniki, Thessaloniki 54124, Greece
[b] Department of Chemistry, University of Crete, Heraklion 71409, Greece
[c] Biocoordination Chemistry Research Group of the Hungarian Academy of Sciences, Department of Inorganic and Analytical Chemistry, University of Szeged, Szeged H-6720, Hungary
[d] Banat University of Agricultural Sciences and Veterinary Medicine, Timisoara 1900, Romania
[e] Department of Chemistry, University of Puerto Rico, Rio Piedras, San Juan, PR 00931-3346, USA
[f] Laboratory of Molecular Analysis, Institute of Organic and Pharmaceutical Chemistry, National Hellenic Research Foundation, Athens 11635, Greece

ARTICLE INFO

Article history:
Received 15 February 2008
Accepted 8 June 2008
Available online 10 August 2008

Keywords:
Aluminum–quinate interactions
Structural speciation
X-ray structure
Solid-state and solution NMR
Aluminum toxicity

ABSTRACT

Efforts to delineate the interactions of Al(III), a known metallotoxin, with low molecular mass physiological substrates involved in cellular processes led to the investigation of the structural speciation of the binary Al(III)–quinic acid system. Reaction of $Al(NO_3)_3 \cdot 9H_2O$ with D-(−)-quinic acid at a specific pH (4.0) afforded a colorless crystalline material $K[Al(C_7H_{11}O_6)_3] \cdot (OH) \cdot 4H_2O$ (**1**). Complex **1** was characterized by elemental analysis, FT-IR, DSC–TGA, ^{13}C-MAS NMR, solution ^{1}H and ^{13}C NMR, and X-ray crystallography. The structure of **1** reveals a mononuclear octahedral complex of Al(III) with three singly ionized quinate ligands bound to it. The three ligand alcoholic side chains do not participate in metal binding and dangle away from the complex. The concurrent study of the aqueous speciation of the binary Al(III)–quinic acid system projects a number of species complementing the synthetic studies on the binary system Al(III)–quinic acid. The structural and spectroscopic data of **1** in the solid state and in solution emphasize its physicochemical properties emanating from the projections of the aqueous structural speciation scheme of the Al(III)–quinic acid system. The employed pH-specific synthetic work (a) exemplifies essential structural and chemical attributes of soluble aqueous species, arising from biologically relevant interactions of Al(III) with natural α-hydroxycarboxylate substrates, and (b) provides a potential linkage to the chemical reactivity of Al(III) toward O-containing molecular targets influencing physiological processes and/or toxicity events.

1. Introduction

Aluminum is an abundant element on the earth's crust with an ostensible presence in a number of abiotic materials. It has long since been recognized, however, as a metallotoxin associated with a number of aberrant cellular processes [1–6]. In humans, its presence has been shown to be linked with neurodegenerative diseases (Alzheimer's disease, microcytic anaemia, encephalopathies, etc.) albeit not through a cause and effect relationship [7–16]. This association is further enhanced by the fact that in an environment progressively being acidified, Al(III) gains access to aquifers and through them to plants, animals and humans.

Once in a cellular milieu, Al(III) interacts with a diverse spectrum of molecular targets varying in size, shape, structure and chemical reactivity. In such a competitive environment, binary and ternary interactions of Al(III) with low and high molecular mass substrates influence its toxicity profile. Among the low molecular mass biotargets of Al(III) are α-hydroxycarboxylic organic acids such as citric acid, malic acid and D-(−)-quinic acid. The latter (a) possesses antimicrobial effects [17], and (b) is an active participant in plant cell metabolism, being a key precursor in the shikimic pathway [18–20]. Through this pathway, essential aromatic amino acids are synthesized, contributing to the maintenance of cell physiology in the plant structure. It also occurs widely in fruit, other than grapes. There, the ester of quinic acid with caffeic acid (chlorogenic acid) is the first line of defense against fungal invasion. Quinic acid is also used as a raw material or building block in the synthesis of new pharmaceuticals currently undergoing clinical trials. It also participates in the photosynthetic process, where the presence of metal ions, in

* Corresponding authors. Tel.: +30 2310 996 179; fax: +30 2310 996 196 (A. Salifoglou).
E-mail address: salif@auth.gr (A. Salifoglou).

0277-5387/$ - see front matter © 2008 Elsevier Ltd. All rights reserved.
doi:10.1016/j.poly.2008.06.029

the form of coordination compounds, modulates the effect of the ligand itself [21]. The structure of quinic acid is that of a polyfunctional natural ligand containing an α-hydroxycarboxylic acid moiety on one side of the molecule and three alcoholic moieties on the other side. Hence, its chemical structure provides efficient anchors to metal ionic targets, exemplified through variable binding modes in a diverse spectrum of metal ionic geometries.

In view of the known accumulation [22–24] and toxicity of Al(III) in plants, animals and humans, its toxic manifestations entail a deep knowledge of its chemistry at the molecular level. Therefore, the aqueous speciation of this metallotoxin in binary and ternary systems, containing readily available cellular targets, is a valuable source of information. Through the aqueous speciation of such Al(III) binary and ternary systems, soluble and potentially bioavailable forms of the metal ion arise with suitable substrate ligands. It is likely that such Al(III) forms participate in molecular processes linked to that metal ion's toxicity. Poised to delineate the molecular chemistry involved in the establishment of Al(III) toxicity in cellular fluids, we launched efforts targeting the interactions of Al(III) with the natural binder D-(−)-quinic acid. To this end, we herein report on (a) the aqueous speciation of the binary Al(III)–quinic acid system, (b) pH-specific synthetic efforts to characterize species projected through the aqueous speciation of the binary Al(III)–quinic acid system, and (c) the association of the physicochemical profile of specific soluble and potentially bioavailable forms of Al(III)–quinate species, with the biological activity of that metal ion.

2. Experimental

2.1. Materials and methods

All experiments were carried out under aerobic conditions. Nanopure quality water was used for all the reactions. $Al(NO_3)_3 \cdot 9H_2O$, $AlCl_3 \cdot 6H_2O$ and quinic acid were purchased from Aldrich. Potassium hydroxide was supplied by Fluka. The Al(III) stock solution used for potentiometric measurements was prepared from recrystallized $AlCl_3 \cdot 6H_2O$ and its metal ion concentration was determined gravimetrically through its oxinate. The stock solution contained 0.1 M HCl to prevent hydrolysis of the metal ion. The exact concentrations of the ligand solution were determined by potentiometric titration, using the Gran method [25].

2.2. Physical measurements

FT-Infrared spectra were recorded on a Perkin Elmer 1760X FT-infrared spectrometer. A ThermoFinnigan Flash EA 1112 CHNS elemental analyser was used for the simultaneous determination of carbon, and hydrogen (%). The analyser is based on the dynamic flash combustion of the sample (at 1800 °C) followed by reduction, trapping, complete GC separation and detection of the products. The instrument is (a) fully automated and controlled by a PC via the Eager 300 dedicated software, and (b) capable of handling solid, liquid or gaseous substances.

A TA Instruments, model Q 600, system was used to run the simultaneous TGA–DSC experiments. The instrument mass precision is 0.1 μg. About 20 mg of sample was placed in an open alumina sample pan for each experiment. High purity helium and air (80/20 in N_2/O_2) were used at a constant flow rate of 100 mL/min, depending on the conditions required for running the experiment(s). During the experiments, the sample weight loss and rate of weight loss were recorded continuously under dynamic conditions, as a function of time or temperature, in the range 30–1000 °C. Prior to activating the heating routine program, the entire system was purged with the appropriate gas for 10 min, at a rate of 400 mL/min, to ensure that the desired environment was established.

2.3. Solid-state NMR

High resolution solid-state ^{13}C magic angle spinning (MAS) NMR spectra were measured at 100.63 MHz on a Bruker MSL400 NMR spectrometer, capable of high power ^{1}H-decoupling. The spinning rate used for the ^{1}H–^{13}C cross polarization and magic angle spinning experiments was 5 kHz at ambient temperature (25 °C). Each solid-state spectrum was the result of the accumulation of 200 scans. The recycle delay used was 4 s, the 90° pulse was 5 μs and the contact time was 1 ms. All the solid-state spectra were referenced to adamantane, which showed two peaks at 26.5 and 37.6 ppm, respectively, and to the external reference of TMS.

2.4. Solution NMR

The samples for solution NMR studies were prepared by dissolving the crystalline complex in D_2O, at concentrations in the range 0.02–0.10 M. The NMR spectra were recorded on a Bruker AM360 (^{13}C) spectrometer. Chemical shifts (δ) are reported in ppm relative to the internal reference, TMS.

2.5. pH-potentiometric measurements

The stability constants of the proton and Al(III) complexes of the title ligand were determined by pH-potentiometric titrations of 25 mL samples in the pH range 2–9 or until precipitation occurred, under a purified argon atmosphere. Care was taken to ensure that titrimetric data were recorded and collected under conditions taking into consideration the kinetically sluggish Al(III). Duplicate titrations were performed. The reproducibility of the titrations was within 0.005 pH units. Titration points obtained when 5 min was not enough to attain pH equilibrium were omitted from the evaluation. The ionic strength was adjusted to 0.2 M with KCl. The temperature was maintained during the measurements at 25 ± 0.1 °C. The titrations were performed with a carbonate-free KOH solution of known concentration (ca. 0.2 M). The ligand concentration was 0.002, 0.004 or 0.008 M and the metal:ligand ratios were 0:1, 1:1, 1:2 or 1:4. All other experimental conditions were the same as in earlier studies [26,27].

The pH was measured with a computer-controlled Molspin titration system elaborated for titrations at low concentrations and a Metrohm 6.0234.100 combined glass electrode, calibrated for hydrogen ion concentration according to Irving et al. [28]. The concentration stability constants $\beta_{pqr} = [M_pA_qH_r]/[M]^p[A]^q[H]^r$ were calculated with the PSEQUAD computer program [29,30]. The uncertainties (3SD values) of the stability constants are given in the parentheses in Table 3. The stability constants used for the hydroxo species of Al(III) were taken from Ref. 30 and are corrected to $I = 0.2$ M using the Davies equation: −5.49 for $[AlH_{-1}]^{2+}$, −13.54 for $[Al_3H_{-4}]^{5+}$, −108.62 for $[Al_{13}H_{-32}]^{7+}$ and −23.40 for $[AlH_{-4}]^{-}$.

2.6. Preparation of the complex $K[Al(C_7H_{11}O_6)_3] \cdot (OH) \cdot 4H_2O$

A quantity of $Al(NO_3)_3 \cdot 9H_2O$ (0.25 g, 0.68 mmol) was placed in a flask and dissolved in 5.5 mL of H_2O. Subsequently, quinic acid (0.39 g, 2.0 mmol) was added slowly with continuous stirring. The solution was heated to 50 °C for 1 h until all of the reagents dissolved, and then it was cooled. Aqueous KOH was then added slowly to adjust the pH to a final value of 4.0. The resulting solution was stirred overnight. The following morning, addition of cold ethanol at 4 °C resulted, after a couple of weeks, in the deposition of a colorless crystalline material. The crystals were isolated by filtration and dried in vacuo. The yield was 0.34 g (~70%). *Anal.* Calc. for **1**, $K[Al(C_7H_{11}O_6)_3] \cdot (OH) \cdot 4H_2O$, $AlC_{21}H_{42}KO_{23}$, M.W. 728.63: C, 34.58; H, 5.76. Found: C, 34.41; H, 5.87%.

3. X-ray crystallography

3.1. Crystal structure determination

X-ray quality crystals of compound **1** were grown from mixtures of water–ethanol solutions. A single crystal, with dimensions 0.26 × 0.22 × 0.20 mm, was mounted on the tip of a glass fiber with epoxy glue. Single crystal analysis was carried out on a Bruker SMART 1K CCD diffractometer. The frame data were acquired with the SMART software [31] using Mo Kα radiation (λ = 0.71073 Å). Final values of the cell parameters were obtained from the least-squares refinement of the positions of 807 reflections. A total of 1271 thirty-second frames were collected in three sets with 0.3° ω-scans. The frames were then processed using the SAINT software [32] to provide the *hkl* file corrected for Lorentz and polarization effects. No absorption correction was applied. Further experimental crystallographic details: for **1**, θ range for data collection = 1.92–23.2°; number of reflections collected/unique/used, 14960/1641[$R_{(int)}$ = 0.0245]/1580; 154 parameters refined; $F(000)$ = 1536; $(\Delta\rho)_{max}/(\Delta\rho)_{min}$ = 0.842/−0.285 e/Å^3; goodness-of-fit = 1.111; R/R_w (for all data), 0.0481/0.1427. Table 1 summarizes the crystallographic structural and refinement parameters.

The structure was solved by direct methods using the SHELX-90 program [33] and refined by least-squares methods on F^2, SHELXL-97 [34], incorporated in SHELXTL, Version 5.1 [35]. The initial E-maps yielded all non-hydrogen atom positions. Hydrogen atoms on carbon atoms were geometrically positioned and left riding on their parent atoms during the structure refinement. Hydrogen atom positions, which belong to water or hydroxyl groups, were first determined from E-maps, brought to reasonable distances from their parent oxygen atoms, and then fixed. The final assignment satisfies electroneutrality for the entire compound, on the premise that the aluminum ions are formally in the oxidation state +3. All non-hydrogen atoms were refined anisotropically.

4. Results and discussion

4.1. Synthesis

The synthesis of compound **1** was pursued through the facile reaction of Al(III) with quinic acid in aqueous media. The pH, at which the reaction was run, was 4.0. The adjustment of the pH was achieved with aqueous KOH. The stoichiometric reaction leading to the isolation of **1** is shown below (Reaction (1)):

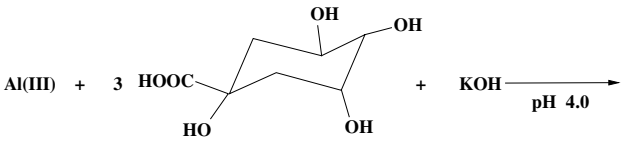

$K[Al(C_7H_{11}O_6)_3]\cdot(OH)$ + 3 H$^+$ Reaction 1

The compound was isolated in the pure crystalline form upon addition of ethanol to the reaction mixture at 4 °C. Elemental analysis of the isolated colorless crystalline material suggested the molecular formulation $K[Al(C_7H_{11}O_6)_3]\cdot(OH)\cdot 4H_2O$. Further spectroscopic inspection by FT-IR revealed the presence of quinates bound to Al(III), thus confirming the aforementioned formulation (**1**).

Compound **1** is soluble in water, but insoluble in organic solvents, like methanol, acetonitrile, chlorinated solvents ($CHCl_3$, CH_2Cl_2), toluene and DMF. The material is stable in air at room temperature for extended periods of time.

4.2. X-ray crystallographic structure of $K[Al(C_7H_{11}O_6)_3]\cdot(OH)\cdot 4H_2O$ (*1*)

The X-ray crystal structure of **1** reveals the presence of a lattice comprised of $[Al(C_7H_{11}O_6)_3]$ units and K^+ ions counteracted by discrete OH^- ions. The compound crystallizes in the cubic space group $P2_13$. The ORTEP diagram along with a perspective view of **1** is shown in Figs. 1 and 2. Selected interatomic distances and bond angles for **1** are listed in Table 2. The structure consists of a mononuclear core unit assembled by a central Al(III) ion surrounded by three quinate ligands. The latter moieties bind to the metal ion through the carboxylate and protonated alcoholic oxygens O(1′) and O(3), respectively. Formation of the Al(III) assembly proceeds through the formation of a five-membered ring, rendering the

Table 1
Summary of Crystal, Intensity Collection and Refinement Data for $K[Al(C_7H_{11}O_6)_3]\cdot(OH)\cdot 4H_2O$ (**1**)

	1
Formula	$C_{21}H_{42}AlKO_{23}$
Formula weight	728.63
T (K)	293(2)
Wavelength	Mo Kα 0.71073
Space group	$P2_13$ (No.198)
a (Å)	15.0093(9)
b (Å)	15.0093(9)
c (Å)	15.0093(9)
α (°)	90
β (°)	90
γ (°)	90
V (Å^3)	3381.3(4)
Z	4
D_{calc}/D_{measd} (Mg m^{-3})	1.431/1.45
Absorption coeffient (μ), mm^{-1}	0.271
Range of h,k,l	−13→19, −16→16, −16→16
Goodness-of-fit on F^2	1.111
R indices[a]	R = 0.0470, R_w = 0.1414[b]

[a] R values are based on F values, R_w values are based on F^2. $R = \frac{\sum||F_o|-|F_c||}{\sum(|F_o|)}$, $R_w\sqrt{\sum[w(F_o^2-F_c^2)^2]/\sum[w(F_o^2)^2]}$.

[b] [1580 refs $I > 2\sigma(I)$].

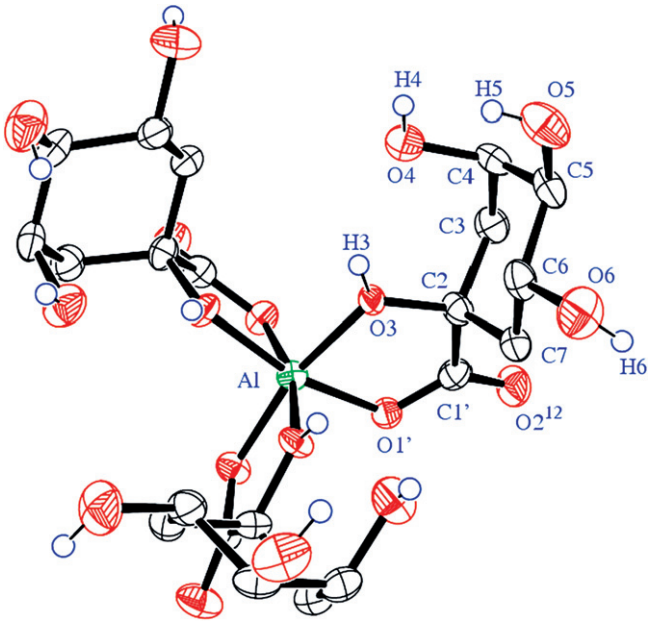

Fig. 1. Labelled ORTEP plot of the $[Al(C_7H_{11}O_6)_3]$ assembly with thermal ellipsoids drawn at the 30% probability level. Hydrogen atoms have been included for alcoholic moieties.

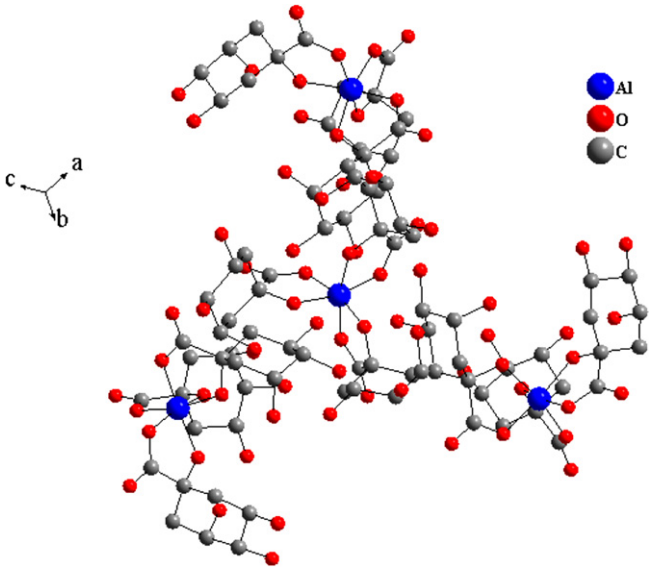

Fig. 2. Perspective view of the arrangement of Al–quinate units along the diagonal of the unit cell.

Table 2
Bond lengths (Å) and angles (°) in $K[Al(C_7H_{11}O_6)_3] \cdot (OH) \cdot 4H_2O$ (**1**)

Distances (Å)	
Al(1)–O(1)	1.876(2)
Al(1)–O(3)	1.891(2)
Angles (°)	
O(1)–Al(1)–O(1)′	90.57(11)
O(1)–Al(1)–O(3)	166.03(9)
O(1)–Al(1)–O(3)′	101.03(10)
O(1)–Al(1)–O(3)″	81.65(9)
O(3)′–Al(1)–O(3)	88.45(11)

Symmetry operation (′): $-y + 3/2, -z + 1, x - 1/2$; (″) $z + 1/2, -x + 3/2, -y + 1$.

arising species quite stable. Therefore, the six coordination sites around Al(III) are taken up by the three quinate ligands bound in the same bidentate fashion. The rest of the alcoholic groups of the quinate ligands do not bind Al(III), dangling away from its coordination sphere. The overall coordination geometry in **1** is distorted octahedral. Charge balance consideration and inspection of the bond lengths of the alcoholic and carboxylate groups indicate that the ligand is singly deprotonated, with the site of deprotonation being the terminal carboxylate group, while the α-alcoholic moiety remains protonated.

The Al–O bond distances in **1** are in line with those in other Al(III) oxygen-containing complexes, like $(NH_4)_5[Al(C_6H_4O_7)_2] \cdot 2H_2O$ (**2**) (1.844(3)–1.961(3) Å) [36], $(NH_4)_4[Al(C_6H_4O_7)(C_6H_5O_7)] \cdot 3H_2O$ (**3**) (1.836(1)–1.959(1) Å) [37], the dinuclear $(NH_4)_4[Al_2(C_6H_4O_7)(C_6H_5O_7)_2] \cdot 4H_2O$ (**4**) (1.835(3)–1.932(3) Å) [38], the trinuclear $(NH_4)_5[Al_3(C_6H_4O_7)_3(OH)(H_2O)] \cdot (NO_3) \cdot 6H_2O$ (**5**) [39] (1.832(5)–1.935(5) Å), and the M(III)–O distances in the congener complexes $(NH_4)_3[Ga(C_2O_4)_3] \cdot 3H_2O$ (1.961–1.976 Å) [40], $(NH_4)_4[Ga(C_6H_4O_7)(C_6H_5O_7)] \cdot 3H_2O$ (1.893(1)–2.058(1) · Å) and $(NH_4)_5[Ga(C_6H_4O_7)_2] \cdot 2H_2O$ (1.902(2)–2.056(2) Å). The Al–O distances are also similar to M(III)–O distances observed in other mononuclear M(III)–hydroxycarboxylate complexes such as $(NH_4)_5[Fe(C_6H_4O_7)_2] \cdot 2H_2O$ (1.953(2)–2.068(2) · Å) [41,42], $(NH_4)_3[Ga(C_6H_5O_7)_2] \cdot 4H_2O$ (1.890(2)–2.054(2) · Å) [43], and $(NH_4)_4[Cr(C_6H_4O_7)(C_6H_5O_7)] \cdot 3H_2O$ (1.933(2)–1.993(2) · Å) [44].

The protonated alcoholic moiety participates in hydrogen bonding interactions. Therefore, the presence of potassium ions along with the discrete OH^- groups in the lattice and the solvent water molecules further stabilizes the above-mentioned network, contributing to the stability of the crystal lattice in **1**.

4.3. FT-IR spectroscopy

The FT-infrared spectrum of **1** in KBr revealed the presence of vibrationally active carboxylate groups. Thus, antisymmetric as well as symmetric vibrations for the carboxylate groups in the coordinated quinate ligand were present in the spectrum. Specifically, antisymmetric stretching vibrations $\nu_{as}(COO^-)$ for the carboxylate carbonyls appeared between 1676 cm^{-1} and 1653 cm^{-1} for **1**. Symmetric vibrations $\nu_s(COO^-)$ for the same groups emerged in the range between 1384 cm^{-1} and 1365 cm^{-1} for **1**. The frequencies of the observed carbonyl vibrations were shifted to lower values in comparison to the corresponding vibrations in free quinic acid, thereby indicating changes in the vibrational status of the quinate ligand upon binding to the Al(III) ion [45]. The difference between the symmetric and antisymmetric stretches, $\Delta(\nu_{as}(COO^-) - \nu_s(COO^-))$, was greater than 200 cm^{-1}, indicating that the carboxylate groups of the quinate ligand were either free or coordinated to Al(III) in a monodentate fashion [46]. The latter contention was subsequently confirmed by the X-ray crystallography. All of the above assignments were in agreement with past observations in mononuclear $Al(III)O_6$ complexes [47], and in line with previous reports on carboxylate-containing ligands bound to metal ions [36,48–55].

4.4. Solid-state NMR spectroscopy

The MAS ^{13}C-NMR spectrum of **1** is consistent with the coordination mode of quinate around the Al(III) ion. The spectrum showed several discrete peak features. Two of those lie in the high field region, whereas the rest lie at lower fields. The two peaks in the high field region (34.4 and 40.7 ppm), were attributed to the C(6) and C(2) carbons, respectively, of the CH_2 groups in the quinate ligands bound to the central Al(III) ion. The resonances at 67.0, 71.3, 74.5 and 79.0 ppm were assigned to the C(5), C(3), C(4) and C(1) carbons, respectively, of the bound quinate. The signal at 180.0 ppm in the lower field region was assigned to the carboxylate carbon C(7) coordinated to the Al(III) central ion. This signal was shifted to lower fields in comparison to the corresponding signal in the free quinic acid. A similar pattern of ^{13}C resonances was observed in the case of mononuclear complexes containing other α-hydroxycarboxylate ligands (i.e. citrate), such as $(NH_4)_5[Al(C_6H_4O_7)_2] \cdot 2H_2O$ [36].

4.5. Solution NMR spectroscopy

The solution ^{13}C NMR spectrum of complex **1** was measured in D_2O (Fig. 3). The spectrum revealed the presence of several resonances. The two resonances in the high field region (38.9 and 43.2 ppm), were attributed to the C(6) and C(2) carbons, respectively, of the CH_2 groups in the quinate ligands bound to the central Al(III) ion. The resonances at 69.7, 74.0, 77.8 and 81.7 ppm were assigned to the C(5), C(3), C(4) and C(1) carbons, respectively, of the bound quinate. The signal at 183.6 ppm in the lower field region was assigned to the carboxylate carbon C(7) coordinated to the Al(III) central ion. This signal was shifted to lower fields in comparison to the corresponding signal in the free quinic acid. The shift was ~1.2 ppm downfield and was comparable to that observed in the MAS ^{13}C solid-state spectrum of **1**. It is worth noting that the pattern of resonances observed was similar to that observed in the solid state ^{13}C-MAS NMR spectrum of **1**. Further inquiry, however, into the solution ^1H NMR spectroscopy of compound **1** in D_2O revealed the presence of free quinate in equilibrium with

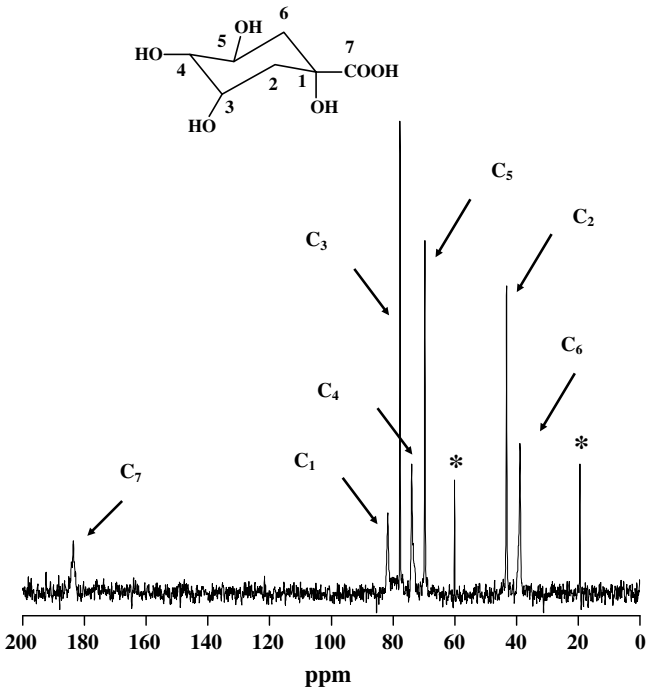

Fig. 3. ^{13}C NMR of **1** in solution (D_2O), at the autogenous pH. The signals marked with a star (*) belong to ethanol from the reaction mixture.

the species under investigation (See Supplementary data). Collectively, the data in solution support the presence of a mononuclear complex like **1,** but not identical in composition with that in the solid state.

4.6. Speciation studies

Potentiometric titrations were carried out on the ligand quinic acid alone and the binary system Al(III)–quinic acid in various metal ion to ligand molar ratios. Quinic acid contains only one dissociable proton in the measurable pH range (pK(HA) = 3.34(2)). The alcoholic hydroxyl groups are very weakly acidic dissociating up to pH ~ 13. For the titratable quinate carboxylate group, the pK_a value of 3.34 was obtained and was found to be very close to the values reported by Clifford (3.40) [56] and Luethy-Krause et al. (3.36) [57]. The obtained metal ion-ligand titration curves were evaluated with different potential speciation models. As quinic acid contains an α-hydroxycarboxylate moiety, the speciation model found for lactic acid [58,59] was tested first. An acceptable fit between the experimental and calculated titration curves for the binary Al(III)–quinic acid system was achieved by considering the species $[Al(H_2O)_6]^{3+}$ (Al), $[AlL]^{2+}$ (LH = $C_7H_{12}O_6$, L = $C_7H_{11}O_6^-$), $[AlLH_{-1}]^+$, $[AlLH_{-3}]^-$, $[AlL_2H_{-1}]^0$, the dinuclear form $[Al_2L_2H_{-4}]^0$, the polynuclear form $[Al_{13}L_4H_{-32}]^{3+}$, and the mononuclear $[AlH_{-4}]^-$ species toward the end of the investigated pH range. The fit was reasonably good in the overall employed pH and concentration range, indicating that the adopted speciation model was satisfactorily defined. Other binary Al(III):quinate complexes, including variably protonated and deprotonated species, were rejected by the computer program (PSEQUAD) during the computational process. The omission of any of the metal–ligand species decreased the fit by at least 30%. Accordingly, it can be stated that the suggested speciation model, with stability constants listed in Table 3, is the best model describing the solution state of the Al(III)–quinate system in the pH and concentration range studied. The uncertainties (3SD values) of the stability constants are given

Table 3
Proton (log$K$) and Al(III)–quinate complex formation constants (logβ) at I = 0.15 M (NaCl) and 25 °C[a]

Species	Quinic acid	logβ	pH range of participating species
	HL ($C_7H_{12}O_6$)	3.34(2)	
Al			2–5.5
AlL		1.84(3)	2–5
$AlLH_{-1}$		−1.05(2)	2–6.5
$AlLH_{-3}$		−11.48(5)	4–9
AlL_2H_{-1}		1.50(8)	2–6.5
$Al_2L_2H_{-4}$		−8.96(9)	4–7
$Al_{13}L_4H_{-32}$		−95.99(14)	5–6.5
AlH_{-4}		−23.4	7–9
Number of points		236	
Fitting parameter[b]		0.0106	

[a] Charges from the various species are omitted for reasons of clarity.
[b] Goodness of fit between the experimental and the calculated titration curves, expressed in mL of titrant.

in parentheses. The pH range of their optimal formation is also reported. The species emerging from the speciation distribution of the binary system are basically in line with the overall structural characteristics encountered in species **1**, which was synthesized and isolated in the solid state. The collective data, however, indicate that the 3 × (COO^-, OH) type six-coordinate octahedral geometry, observed in the solid state species **1**, does not persist in solution in the whole pH range up to neutral pH.

On the basis of the analytical and crystallographic data, the alcoholic group of the quinate retains its proton upon binding to Al(III). Thus, there is no expected pH-dependence of the deprotonation of that group and the specific mode of binding to Al(III) over the investigated pH range. However, it has been proven by pH-potentiometric, NMR and CD spectroscopic methods that Al(III) may induce deprotonation of the weakly acidic alcoholic-OH group in various α-hydroxycarboxylic acids (such as lactic acid, malic acid, citric acid) [60,61]. The titration curves in the absence and presence of Al(III) suggest clearly formation of the mononuclear 1:1 complexes $[Al(H_2O)_6]^{3+}$, $[AlL]^{2+}$ and $[AlLH_{-1}]^+$, and the 1:2 complex $[AlL_2H_{-1}]^0$ in the acidic region up to pH 5. In the early part of that range, the predominant species is $[Al(H_2O)_6]^{3+}$. The latter three species $[AlL]^{2+}$, $[AlLH_{-1}]^+$ and $[AlL_2H_{-1}]^0$ contain a singly deprotonated quinate ligand bound to Al(III). As the pH of the aqueous solution increases from 2 to 5, the fraction of the mononuclear species such as $[AlL]^{2+}$, $[AlLH_{-1}]^+$ and $[AlL_2H_{-1}]^0$ increases progressively. Around pH 4.5, the predominant species is $[AlLH_{-1}]^+$. Towards the end of the specific pH range, new species such as the mononuclear $[AlLH_{-3}]^-$, and the dinuclear form $[Al_2L_2H_{-4}]^0$ arise.

In the pH range 5–7, three species emerge, namely $[AlLH_{-3}]^-$, $[Al_2L_2H_{-4}]^0$ and the polynuclear cluster form $[Al_{13}L_4H_{-32}]^{3+}$. In the pH range 5–5.5, the predominant species is the dinuclear species $[Al_2L_2H_{-4}]^0$, gradually growing in from the latter part of the previously described pH range and reaching a maximum around 5.2. Slowly emerging in the same pH range is the mononuclear $[AlLH_{-3}]^-$ species, which eventually predominates over the entire range of values beyond 5.5. Slightly above that pH value, a polynuclear assembly of Al(III) ions bound to quinates, namely $[Al_{13}L_4H_{-32}]^{3+}$, emerges as a participant, albeit at a minor fraction compared to the other two species. In a fashion similar to the Al(III)–lactic acid system, what was suggested as $[Al_2L_2H_{-4}]^0$ and $[Al_{13}L_4H_{-32}]^{3+}$ are oligo(poly)nuclear hydroxo species [58,59].

Albeit not definitively proven, it is worth noting that the dinuclear species $[Al_2L_2H_{-4}]^0$ may originate from the previously emerging $[AlLH_{-1}]^0$ species, for which a clear picture of the coordination mode of quinate was proposed. On these grounds, dinuclear com-

plex formation through the mononuclear species as a synthon could be perceived to proceed through (a) employment of the coordinated quinate carboxylate group binding to an adjacent $[AlLH_{-1}]^+$ species unit (and vice versa) through the second oxygen anchor, (b) utilization of the alcoholic moiety as a bridge between abutting $[AlLH_{-1}]^+$ units, and (c) deprotonation of coordinated water molecule(s) leading to OH^- moieties potentially acting as template bridges to the adjacently located $[AlLH_{-1}]^+$ units. Thus, hydroxo bridged dinuclear assembly formation could be promoted. This thesis is consistent with the fact that hydroxo and dihydroxo bridges are a characteristic feature in Al(III) complexation chemistry, leading to dinuclear species in the solid state. Representative examples of such species are complexes of trivalent metal ions such as $[(Al_3(C_6H_4O_7)_2(OH)_2(H_2O)_4]_2 \cdot (NO_3) \cdot 6H_2O$ [62], $Na_6[Al_6(C_6H_6O_8)_4(OH)_8] \cdot 21H_2O$ [63], $[Al_{13}(\mu_3\text{-}OH)_6(\mu_2\text{-}OH)(C_6H_8NO_5)_6(H_2O)_6] \cdot (NO_3)_3$ [64], and $[Al_2(OH)_2(C_4H_5NO_4)_2(H_2O)_2]$ [65], and Cr(III) i.e. $([(H_2O)_4Cr(OH)_2Cr(H_2O)_4]^{4+}$ [66,67], $[Cr(tpa)(OH)]_2(ClO_4)_4\ 4H_2O$ [68], $[Cr(gly)_2(OH)]_2$ [69,70] and $[Cr(pic)_2(OH)]_2^{4+}$ [71]), already reported in the literature. Analogous chemistry has been observed in the case of Cu(II) and VO(II). On similar grounds, all of these metal ions were shown to be able to induce deprotonation of the weakly acidic alcoholic-OH function in various hydroxyl group derivatives when the OH group lies adjacent to another strongly coordinating donor group [58,59,72–74].

What emerges as a noteworthy observation from the aqueous speciation scheme is the 1:1 and 1:2 Al(III):quinate stoichiometry for the majority of the species present in it. In both cases of Al(III):quinate ratios, the binding mode of the quinate ligand(s) could be either through the carboxylate group or through the carboxylate and α-alcoholate groups, while the remaining polyol functionalities do not enter the coordination sphere of Al(III). It appears that the bidentate coordination of α-hydroxycarboxylate containing ligands through carboxylate groups may also be preferred in other divalent or trivalent metal ions, such as Cu(II) [72], Co(II) [75], Al(III)[73] and VO(II) [74]. Accordingly, it is very probable that the deprotonated species between Al(III) and quinic acid form isomeric structures and the coordination sphere of the metal ion is filled by monodentate or bidentate bound quinate, hydroxo and water ligands. The additional H_{-1} in species, such as $[AlLH_{-1}]^+$, $[AlL_2H_{-1}]^0$, could emerge upon dissociation of the α-OH group and coordination of the incipient α-O^- group or dissociation of a coordinated water molecule from $[AlL]^{2+}$ and $[AlL_2]^+$. Considering the data in this pH range, it appears that $\log K(AlL_2H_{-1})$ (characteristic for the equilibrium $AlLH_{-1} + L \rightleftarrows AiL_2H_{-1}$) is 2.55 and is similar to the $\log K(AlL)$ value of 1.84, indicating that only one ligand molecule is coordinated via a deprotonated alcoholate. The second ligand is bound to Al(III) in a (COO^-, OH) fashion. This value also indicates favorable formation for $[AlL_2H_{-1}]^0$ over that of $[AlLH_{-1}]^+$, due to charge neutralization. As a matter of fact, the two species coexist in the same pH range, with the former species comprising 30% of the total Al(III) fraction compared to ~50% for the latter species at pH ~ 4.5 (Fig. 4).

In the high pH zone, from 7 to 9, the two species present are $[AlLH_{-3}]^-$ and $[AlH_{-4}]^-$, both mononuclear in nature. In the first case, the mixed hydroxo $[AlLH_{-3}]^-$ species might exhibit isomeric binding modes. To this end, one formulation could include a singly deprotonated quinate, three hydroxides originating from the deprotonation of an equivalent number of bound water molecules, with the coordinated quinate preventing precipitation of $Al(OH)_3$ [76]. In the other binding mode, quinate coordinates in a bidentate (COO^-, O^-) fashion and only two OH^- ions are ionized in the coordination sphere of the metal ion. The $[AlLH_{-3}]^-$ species is the only species present around pH 7 and is the predominant species of the physiological pH range and even beyond that. The second species, $[AlH_{-4}]^- = [Al(OH)_4]^-$ ($\log\beta_{1-4} = -23.4$), emerges as a minor tetrahedral Al(III) species after pH 7 and reaches a maximum of 35% of the total fraction of Al(III) toward the high end of the investigated pH range. In a fashion similar to the Al(III)–lactate system, polynuclear species such as $Al_2L_2H_{-4}$ and $Al_{13}L_4H_{-32}$ also form in the pH range 4–7, in a significant but lower concentration than in the former system, probably due to the larger spatial requirement of the quinate ligand.

4.7. Thermal studies

The thermal decomposition of the title complex was studied by TGA–DSC under an atmosphere of oxygen (Fig. 5). The complex $K[Al(Quinic)_3] \cdot (OH) \cdot 4H_2O$ (**1**) is thermally stable up to 30 °C. From that point on, a fairly broad heat process points to the dehydration of **1**, with the release of lattice water molecules between 30 and 180 °C, signifying an endothermic process. The observed weight loss amounts to 9.63%, a value close to the calculated value of 9.88% based on the molecular formula of the title complex. Beyond the specific temperature, it appears that the quinate ligand loses its integrity. In a second step, the release of carbon dioxide is observed from the compound between 180 °C and 225 °C. The observed weight loss amounts to 6.13%, a value very close to the calculated value of 6.04% based on the molecular formula of the title complex. Subsequently, consecutive steps ensue between 225 and 500 °C that are associated with further decomposition of the organic part of the molecule. No clear plateaus are reached in these stages, suggesting that the derived products are unstable and

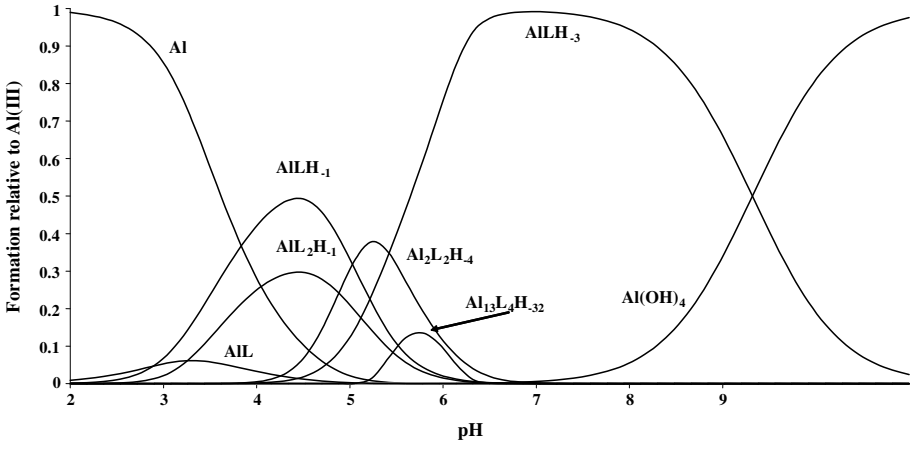

Fig. 4. Speciation curves for complexes forming in the Al(III)–quinic acid system; c_{Al} = 0.001 mol dm^{-3}, c_{ligand} = 0.003 mol dm^{-3}. Charges are omitted for clarity.

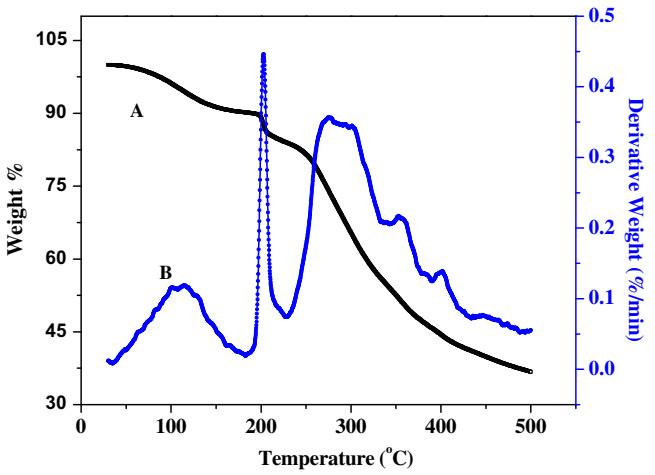

Fig. 5. TGA (A) and DSC (B) analysis of **1**.

decompose further. The total weight loss of 86.8% due to the decomposition of the title complex is reached at 518 °C, with no further loss up to 800 °C. This value is in good agreement with the calculated weight loss derived upon the thesis that the product at that temperature (500 °C) is Al_2O_3. The DSC profile of the complex exhibits clear features that correspond to the aforementioned TGA processes. Collectively, the specified number of observed processes very likely reflects discrete mechanistic steps for the decomposition pathways of **1**.

5. Discussion

5.1. A closer look at the aqueous Al(III)–quinic acid chemistry

As a metallotoxin, Al(III) has been linked to a number of pathological conditions in plants (soil acidity complex) [77] and humans (Alzheimer's disease) [11,12,16]. In both cases, its cellular toxicity entails a diverse aqueous chemistry at the molecular level, that, in turn, is linked to the existence of soluble and bioavailable forms of that metal ion influencing its chemical reactivity. To this end, understanding Al(III) toxicity is closely tied to well-characterized soluble forms of Al(III) that can promote its reactivity with physiological targets through ensuing ternary interactions. Drawn by the paucity of such well-defined forms of Al(III) in aqueous media that promote interactions leading to aberrant cellular (neuro)physiologies, a structural speciation approach was adopted encompassing pH-dependent synthetic reactions between Al(III) and the physiological substrate D-(−)-quinic acid. At the optimally established pH 4, the new binary species $K[Al(C_7H_{11}O_6)_3]\cdot(OH)\cdot 4H_2O$ (**1**) arose and was isolated in a pure crystalline form. The physicochemical characterization of **1** projected structural and chemical properties relating to the following:

(a) The arisen aqueous chemistry in this binary system under the employed conditions is linked to the formation of discrete complexes of Al(III) bearing quinate ligands. The specificity of the reaction pH was crucial in deriving the new material in a pure and crystalline form. pH-specific synthesis had previously been successfully applied in the case of soluble metal-hydroxycarboxylate species involving trivalent (Al(III), Ga(III), Fe(III)) [36,37,41] and divalent metal ions (Co(II), Mn(II)) [49,50].

The physicochemical properties of **1** contribute significantly to understanding its nature both in the solid state and in solution (*vide infra*). In this regard, delineation of the composition of the coordination sphere of Al(III) in solution reflects distinct structural features on species arising from the interaction of the metal ion with natural O-containing low molecular mass substrates in biologically relevant media. The fact that in solution species such as $[AlL_2]^+$ or $[AlL_2H_{-1}]^0$ may arise consolidates further the emergence of Al(III)–O_6 moieties (very likely octahedral, albeit not unequivocally delineated as such by NMR beyond pH 4–5 due to parallel formation of $Al(OH)_3$) in aqueous media through binary and ternary interactions of Al(III) with O-containing targets. The so arisen interactions could reflect a general multifactorial contribution to $[AlL_2]^+$ or $[AlL_2H_{-1}]^0$ emergence as a speciation participant, primarily influenced by factors such as pH, ligand deprotonation state, H-bond formation and others. Along with the thermal behavior, the overall data formulate a well-defined physicochemical profile for **1**, supporting its solid-state nature and its solution signature.

(b) The structural characterization of **1** reveals distinct traits of the interaction between Al(III) and quinic acid. Firstly, the mode of coordination of the ligand with the metal ion is specific and derives from the propensity of the α-hydroxycarboxylate moiety to promote metal ion binding. A key factor driving this particular reactivity of Al(III) is the formation of stable five-membered rings for the quinate ligands bound to Al(III). Secondly, the employment of the alcoholic moiety of the α-hydroxycarboxylate group to bind Al(III) is marked by a retention of the proton on the specific oxygen (as evidenced by the solid-state structure of the isolated species **1**). The aqueous speciation work, however, provides further insight into the chemical behavior of the quinate ligand anchored to Al(III). Specifically, both singly ionized quinate as well as doubly ionized quinate moieties appear to anchor to Al(III), giving rise to binding isomers for specific species such as $[AlLH_{-1}]^+$ and $[AlL_2H_{-1}]^0$. This behavior may imply similarities to the aqueous Al(III) chemistry at pH values lower or higher than the one employed here, or to the chemistry of other divalent/trivalent metal ions with the same ligand. In no cases so far, however, have doubly deprotonated quinate-containing mononuclear octahedral metal complexes been synthesized and isolated, thus projecting the interconnection of the inherent chemical properties of the various metal ions with the complexity and diversity of species present in aqueous media. To this end, the possibility that the Al(III)–quinate binary system would give rise to new, thus far elusive, species in a pH-dependent fashion cannot be discounted.

(c) The three alcoholic groups almost diametrically located with respect to the α-hydroxycarboxylate moiety play totally different roles. They do not participate in the formation of five-member metallacyclic rings, like the α-hydroxycarboxylate moiety does, which further stabilizes the entire mononuclear complex. In the case of divalent metal ions, such as Mn(II) [78], participating in binary systems with quinic acid, the terminal alcoholic moieties were variably involved in the formulation of the coordination sphere of the metal ion, differentiating the structural environment of abutting Mn(II) ions in the arising solid-state lattice, without losing their protons. Specifically, one of the polyolic group members acts as a bridge between adjacently located metal ion centers, leading to the formation of dinuclear species $[Mn_2(C_7H_{11}O_6)_4]_n\cdot nH_2O$ infinitely extended in a polymeric and molecular lattice. Even though that behavior was observed in the crystalline state only, it projects the potential affinity of polyol functionalities for metal ion coordination, such as Al(III), as ligand terminals on diverse physiological substrates interacting with it in biologically relevant fluids.

5.2. Correlation of structural diversity in the aqueous binary Al(III)–quinate speciation with the synthetic chemistry

The aqueous speciation in the binary Al(III)–quinic acid system (Fig. 4) can be described satisfactorily by considering the presence of (a) 1:1 Al(III)–quinate complexes in the form $[AlL_n(H_{-1})_p]^{q+}$ ($n = 0$, $p = 0$, q = 3; $n = 1$, $p = 1$, q = 1; $n = 1$, $p = 0$, $q = 2$), the neutral $[AlL_2H_{-1}]^0$ and dinuclear $[Al_2L_2H_{-4}]^0$ forms, the anionic

$[AlL_n(H_{-1})_p]^{q-}$ ($n = 0$, $p = 4$, $q = 1$; $n = 1$, $p = 3$, $q = 1$) and polynuclear $[Al_{13}L_4H_{-32}]^{3+}$ forms, and (b) 1:2 mononuclear Al(III)–quinate species $[AlL_2H_{-1}]^0$.

On the basis of the aforementioned observations, it is logical to juxtapose the results of the aqueous speciation with the solid-state structure of compound **1** and its physicochemical properties in the solid state and in solution. To that end, the solid-state structure of **1** suggests the existence of an octahedral Al(III) central metal ion surrounded by three singly deprotonated quinate ligands, thus filling all of the six available coordination sites. In solution, the NMR data obtained for **1** upon dissolution and at the equilibrium state suggest that (a) the species does not retain its solid-state structure in solution, thereby releasing quinate away from the coordination sphere of Al(III), and (b) even the binding mode of the quinate may change from (COO^-, OH) to (COO^-, O^-) coordination. Consistent with this general behavior is the suggestion offered by the aqueous speciation that, in the pH range investigated synthetically, there are two species prevailing. These are $[AlLH_{-1}]^+$ and $[AlL_2H_{-1}]^0$. Consequently: (a) the fact that **1** has been isolated in the solid state with the specific molecular lattice composition and physicochemical properties reflects the lattice dynamics of Al(III)–quinate complexation in the solid state, and (b) $[AlL_2H_{-1}]^0$ might be the species that **1** dissociates to upon dissolution in water at the autogenous pH (consistent with the pH range at which the synthesis of **1** was pursued).

The aforementioned remarks lend further credence to the notion that $[AlL_2H_{-1}]^0$, a zero-valent complex (like **1**), is likely the arising species in solution consistent with the potential reactions shown below:

$$[AlL_3]^0 \rightleftarrows [AlL_2]^+ + L^-$$

$$[AlL_2]^+ \rightleftarrows [AlL_2H_{-1}]^0 + H^+$$

To a first approximation, dissociation of $[AlL_3]^0$ to $[AlL_2]^+$ is followed by further deprotonation of one of the Al(III)–bound water molecules, or one of the α-OH groups of the quinate molecules, leading to the formation of $[AlL_2H_{-1}]^0$. Thus, (a) the mononuclear octahedral complex, isolated in the solid state, affords upon dissolution another mononuclear, presumably octahedral complex, containing fewer quinates (two), (b) the charge of $[AlL_3]^0$ (**1**) in the solid state (zero) is maintained upon dissolution of the complex and the formation of the emerging complex $[AlL_2H_{-1}]^0$. The chemical and potential biological repercussions of that property could be relevant to molecular mechanisms of Al(III) toxicity.

From a structural point of view, the quinate ligand is configured so as to promote formation of variable size species extending from low molecular mass complexes to high molecular mass aqueous assemblies. In analogy to other α-hydroxycarboxylate metal ion binders, such as lactic acid, citric acid, malic acid, etc., a chemistry of such breadth would be expected to afford dinuclear and potentially multinuclear Al(III)–quinate clusters. Consistent with this notion is the suggestion offered by the aqueous speciation distribution of this binary system that the dinuclear complex $[Al_2L_2H_{-4}]^0$ exists in the pH range 4–7 and a higher nuclearity cluster $[Al_{13}L_4H_{-32}]^{3+}$ is present in the pH range 5–6.5. With regard to the binding mode of the di- and polynuclear species, the most likely assumption concerning the $Al_2L_2H_{-4}$ complex would be the tentative formula $[Al_2(OH)_2(H_{-1}L)_2]^0$, i.e. a dihydroxo-bridged species in which both quinate ions are doubly deprotonated and bound in a bidentate fashion around the $Al_2(OH)_2$ core. A similar core structure has been reported in $[Al_2(\mu\text{-}OH)_2(\text{nitrilotriacetate})_2]^-$ [79]. Concerning the high-nuclearity species $Al_{13}L_4H_{-32}$, we have no clear suggestion as to the binding mode of quinate in this species. It should be mentioned, however, that for a similar polynuclear species bearing the hydrolytic $[Al_{13}O_4(OH)_{24}]^{7+}$ core and thought to arise upon interaction of Al(III) with lactate, ^{27}Al NMR studies by Marklund and Öhman [58] concluded that in fact the species was not a complex to which lactate ions were coordinated. These assumptions are consistent with the existence of structural features not unlike those encountered in (1) dinuclear oxo- or hydroxo-bridges seen in species such as $K_2[Cr_2(C_6H_6NO_6)_2(OH)_2]\cdot 6H_2O$ [80], $Ba[\{Fe(nta)(H_2O)\}_2O]\cdot 4H_2O$ [81], $[Ga(heidi)(H_2O)]_2$ [82], $[Al(heidi)(H_2O)]_2$ [64] and $[Fe(heidi)(H_2O)]_2$ [83,84], which have been synthesized and isolated, and (2) polynuclear species that could emerge from the herein investigated binary system. As to the latter category of species, the importance of the M:ligand ratio in achieving high nuclearity species has been noted as a key factor in the chemistry of a number of trivalent metal ions like Fe(III), Al(III), Ga(III) and others. Thus, species such as $[Fe_{19}(\mu_3\text{-}O)_6(\mu_3\text{-}OH)_6(\mu_2\text{-}OH)_8(heidi)_{10}(H_2O)_{12}]^+$, $[Fe_{17}(\mu_3\text{-}O)_4(\mu_3\text{-}OH)_6(\mu_2\text{-}OH)_{10}(heidi)_8(H_2O)_{12}]^{3+}$ [83], $[Al_{13}(\mu_3\text{-}OH)(\mu_2\text{-}OH)_{12}(heidi)_6(H_2O)_6]^{3+}$ [64], $[Ga_8(\mu_3\text{-}OH)(\mu_2\text{-}OH)_8(heidi)_4(H_2O)_4(py)_2]^{2+}$ [82] and $[Ga_{13}(\mu_3\text{-}OH)(\mu_2\text{-}OH)_{12}(heidi)_6(H_2O)_6]^{3+}$ [82] have been synthesized. On the basis of the above remarks, pertinent synthetic and physicochemical studies are currently in progress in our lab to complement the already conducted aqueous speciation studies.

5.3. From the aqueous chemistry of the binary Al(III)–quinate system to toxicity

Aside from humans, most plants are fairly sensitive to Al(III) toxicity, a major factor affecting significantly crop productivity in agriculture [77,85] around the world. Therefore, essential in understanding the toxicity of Al(III) at the cellular level, is an in-depth knowledge of the (bio)chemistry of that metal ion with intracellular and/or extracellular targets of variable mass and distinct biological activity. A key contributor to that knowledge is (a) the aqueous speciation of binary/ternary systems of a kinetically sluggish Al(III) with its elicited targets as a function of pH and molecular stoichiometry, and (b) the structure and properties of soluble and bioavailable species of Al(III)–L (substrate) species partaking of the requisite speciation [86]. To this end, the herein described complex **1** is a good example of a species, which (a) in the solid state contains the key physicochemical characteristics of an efficient metal ion binder (ligand to metal ratio, structural features, etc.) anchored onto Al(III), as previously proposed for plant tea organic acids interacting with that metal ion [87,88], (b) in solution, turns into mononuclear Al(III) species bearing a variable metal:ligand ratio while concurrently retaining the overall solid-state characteristics of the binary species, and (c) gives rise to $[AlL_2H_{-1}]^0$, bearing a net neutral charge, presenting a soluble Al(III) entity poised to traverse cellular structures (e.g. membranes) and participate in further chemical reactivity by eliciting interactions from variable mass and structure cellular targets involved in cytosolic and nuclear processes (i.e. cellular-neuronal integrity, degeneration, etc.). Further synthetic chemistry targeting such well-defined yet elusive aqueous Al(III)–quinate pH-structural variants, components of the speciation of that binary system, are under way.

6. Conclusions

The work presented here, projects the nature of the aqueous interactions between Al(III) and a natural O-containing substrate, ultimately leading to well-defined complexes in the solid state and in solution. Both the aqueous speciation study and the invoked synthetic approaches offer invaluable data adumbrating the profile of soluble species in the binary Al(III)–quinate system through the correlation of their structural properties in those two phases. Given the importance of binary and ternary interactions of Al(III) with variable mass cellular targets, understanding the nature and physicochemical properties of **1** in the solid state and in solution is the first step in the delineation of the complex distribution of Al(III)–

quinate species and any related Al(III)–(O-substrate) interactions under conditions dictated by cellular environmental factors and biological settings [89]. Undoubtedly, the contribution of the pH-dependent synthetic chemistry to the investigation of (a) the molecular processes involving this otherwise kinetically sluggish Al(III), and (b) the relationships to molecular neuro(toxic) effects in higher organisms and humans, is significant. To the degree that soluble and bioavailable Al(III)-bound (α-hydroxy)carboxylate-containing biological targets, such as $[AlL_2H_{-1}]^0$, are likely involved in chemical processes underlying (neuro)toxic effects in biological media, further synthetic and solution studies on this specific, as well as other hydroxycarboxylate-bearing binary systems, are expected to shed light on their nature. Work along these lines is currently in progress in our labs.

Acknowledgments

This work was supported by a "Pythagoras" grant from the National Ministry of Education and Religious Affairs, and by a "PENED" grant co-financed by the E.U. European Social Fund (75%) and the Greek Ministry of Development-GSRT (25%), and by the Hungarian Research Fund (OTKA No. NI61786).

Appendix A. Supplementary data

CCDC 678110 contains the supplementary crystallographic data for $K[Al(C_7H_{11}O_6)_3] \cdot (OH) \cdot 4H_2O$ (**1**). These data can be obtained free of charge via http://www.ccdc.cam.ac.uk/conts/retrieving.html, or from the Cambridge Crystallographic Data Centre, 12 Union Road, Cambridge CB2 1EZ, UK; fax: (+44) 1223-336-033; or e-mail: deposit@ccdc.cam.ac.uk. Supplementary data associated with this article can be found, in the online version, at doi:10.1016/j.poly.2008.06.029.

References

[1] P. Nayak, Environ. Res. 89 (2002) 101.
[2] A. Campbell, E.Y. Yang, M. Tsai-Turton, S.C. Bondy, Brain Res. 933 (2002) 60.
[3] V. Rondeau, Rev. Environ. Health 17 (2002) 107.
[4] H. Meiri, E. Banin, M. Roll, A. Rouesseau, Prog. Neurobiol. 40 (1993) 89.
[5] G.B. Van der Voet, M.F. Van Ginkel, F.A. de Wolff, Toxicol. Appl. Pharm. 99 (1989) 90.
[6] D.N.S. Kerr, M.K. Ward, in: H. Sigel, A. Sigel (Eds.), Metal Ions in Biological Systems, vol. 24, Marcel Dekker, Inc., New York, NY, 1988, p. 217 (Chapter 6).
[7] H.H. Malluche, Nephrol. Dial. Transplant. 17 (Suppl. 2) (2002) 21.
[8] J.B. Cannata-Andia, J.L. Fernandez-Martin, Nephrol. Dial. Transplant. 17 (Suppl. 2) (2002) 9.
[9] D. Pratico, K. Uryu, S. Sung, S. Tang, J.Q. Trojanowski, V.M. Lee, FASEB J. 16 (2002) 1138.
[10] M.J. Hull, J.L. Abraham, Hum. Pathol. 33 (2002) 819.
[11] C. Exley, J. Alzheimer's Dis. 3 (2001) 551.
[12] V. Rondeau, D. Commenges, in: C. Exley (Ed.), Aluminium and Alzheimer's Disease: The Science that Describes the Link, Elsevier Science, New York, 2001.
[13] V. Rondeau, D. Commenges, H. Jacqmin-Gadda, J.-F. Dartigues, Am. J. Epidemiol. 152 (2000) 59.
[14] G.D. Fasman, C.D. Moore, Proc. Natl. Acad. Sci. USA 91 (1994) 11232.
[15] M. Clauberg, J.G. Joshi, Proc. Natl. Acad. Sci. USA 90 (1993) 1009.
[16] C. Exley, J.D. Birchall, J. Theor. Biol. 159 (1992) 83.
[17] D. Stead, Lett. Appl. Microbiol. 18 (1994) 112.
[18] E. Haslam, Shikimic Acid: Metabolism and Metabolites, Wiley & Sons, NY, 1993.
[19] A.J. Pittard (Ed.), *Escherichia coli* and Salmonella: Cellular and Molecular Biology, ASM Press, Washington, DC, 1996.
[20] R. Bentley, Crit. Rev. Biochem. Mol. Biol. 25 (1990) 307.
[21] S.E. Castillo-Blum, N. Barbra-Behrens, Coord. Chem. Rev. 196 (2000) 3.
[22] G.E. Hutchinson, Quart. Rev. Biol. 18 (1943) 1.
[23] T. Watanabe, M. Osaki, T. Yoshihara, T. Tadano, Plant Soil 201 (1998) 165.
[24] T.P. Flaten, Coord. Chem. Rev. 228 (2002) 385.
[25] G. Gran, Acta Chem. Scand. 4 (1950) 559.
[26] D. Sanna, G. Micera, P. Buglyo, T. Kiss, J. Chem. Soc., Dalton Trans. (1996) 87.
[27] M. Dyba, M. Jezowska-Bojczuk, E. Kiss, T. Kiss, H. Kozlowski, Y. Leroux, D. El Manouni, J. Chem. Soc., Dalton Trans. (1996) 1119.
[28] H.M. Irving, M.G. Miles, L.D. Petit, Anal. Chim. Acta 38 (1967) 475.
[29] L. Zekány, I. Nagypál, in: D. Leget (Ed.), Computational Methods for the Determination of Stability Constants, Plenum, New York, 1985.
[30] L.O. Öhman, S. Sjöberg, Acta Chem. Scand. 36 (1982) 47.
[31] SMART-NT Software Reference Manual, Version 5.059, Bruker AXS, Inc., Madison, WI, 1998.
[32] SAINT+Software Reference Manual, Version 6.02, Bruker AXS, Inc., Madison, WI, 1999.
[33] G.M. Sheldrick, SHELXS-90, Program for the Solution of Crystal Structure, University of Göttingen, Germany, 1986.
[34] G.M. Sheldrick, SHELXL-97, Program for the Refinement of Crystal Structure, University of Göttingen, Germany, 1997.
[35] SHELXTL-NT Software Reference Manual, Version 5.1, Bruker AXS, Inc., Madison, WI, 1998.
[36] M. Matzapetakis, C.P. Raptopoulou, A. Terzis, A. Lakatos, T. Kiss, A. Salifoglou, Inorg. Chem. 38 (1999) 618.
[37] M. Matzapetakis, M. Kourgiantakis, M. Danakali, C.P. Raptopoulou, A. Terzis, A. Lakatos, T. Kiss, I. Banyai, L. Iordanidis, T. Mavromoustakos, A. Salifoglou, Inorg. Chem. 40 (2001) 1734.
[38] M. Dakanali, C.P. Raptopoulou, A. Terzis, A. Lakatos, I. Banyai, T. Kiss, A. Salifoglou, Inorg. Chem. 42 (2003) 252.
[39] T.L. Feng, P.L. Gurian, M.D. Healy, A.R. Barron, Inorg. Chem. 29 (1990) 408.
[40] N. Bulc, L. Golic, J. Siftar, Acta Crystallogr., Sect. C 40 (1984) 1829.
[41] M. Matzapetakis, C.P. Raptopoulou, A. Tsohos, B. Papefthymiou, N. Moon, A. Salifoglou, J. Am. Chem. Soc. 120 (1998) 13266.
[42] I. Shweky, A. Bino, D.P. Goldberg, S.J. Lippard, Inorg. Chem. 33 (1994) 5161.
[43] P. O'Brien, H. Salacinski, M. Motevalli, J. Am. Chem. Soc. 119 (1997) 12695.
[44] C. Gabriel, C.P. Raptopoulou, A. Terzis, V. Tangoulis, C. Mateescu, A. Salifoglou, Inorg. Chem. 46 (2007) 2998.
[45] G.B. Deacon, R. Philips, J. Coord. Chem. Rev. 33 (1980) 227.
[46] C. Djordjevic, M. Lee, E. Sinn, Inorg. Chem. 28 (1989) 719.
[47] K. Nakamoto, Infrared and Raman Spectra of Inorganic and Coordination Compounds, 5th ed., John Wiley and Sons, Inc., New York, 1997 (Part B).
[48] P. Panagiotidis, E.T. Kefalas, C.P. Raptopoulou, A. Terzis, T. Mavromoustakos, A. Salifoglou, Inorg. Chim. Acta 361 (2008) 2210.
[49] M. Matzapetakis, M. Dakanali, C.P. Raptopoulou, V. Tangoulis, A. Terzis, N. Moon, J. Giapintzakis, A. Salifoglou, J. Biol. Inorg. Chem. 5 (2000) 469.
[50] M. Matzapetakis, N. Karligiano, A. Bino, M. Dakanali, C.P. Raptopoulou, V. Tangoulis, A. Terzis, J. Giapintzakis, A. Salifoglou, Inorg. Chem. 120 (2000) 4044.
[51] W.P. Griffith, T.D. Wickins, J. Chem. Soc. A (1968) 397.
[52] N. Vuletic, C. Djordjevic, J. Chem. Soc., Dalton Trans. (1973) 1137.
[53] M. Kaliva, T. Giannadaki, C.P. Raptopoulou, V. Tangoulis, A. Terzis, A. Salifoglou, Inorg. Chem. 40 (2001) 3711.
[54] M. Tsaramyrsi, D. Kavousanaki, C.P. Raptopoulou, A. Terzis, A. Salifoglou, Inorg. Chim. Acta 320 (2001) 47.
[55] M. Matzapetakis, M. Kourgiantakis, M. Dakanali, C.P. Raptopoulou, A. Terzis, A. Lakatos, T. Kiss, I. Banyai, L. Iordanidis, T. Mavromoustakos, A. Salifoglou, Inorg. Chem. 40 (2001) 1734.
[56] M. Clifford, Tea Coffee Trade J. 159 (1987) 35.
[57] B. Luethy-Krause, I. Pfenninger, W. Landolt, Trees – Struct. Func. 4 (1990) 198.
[58] E. Marklund, L.O. Öhman, Acta Chem. Scand. 44 (1990) 228.
[59] T. Kiss, I. Sóvágó, R.B. Martin, J. Pursiainen, J. Inorg. Biochem. 55 (1994) 53.
[60] R.B. Martin, in: Aluminium in Biology and Medicine, Ciba Foundation Symposium 169, Wiley, Chichester, 1992, p. 5. and references cited therein.
[61] T. Kiss, E. Farkas, Perspect. Bioinorg. Chem. 3 (1996) 199. and references cited therein.
[62] S.A. Malone, P. Cooper, S.L. Heath, Dalton Trans. (2003) 4572.
[63] P. Klufers, G. Kramer, H. Piotrowski, J. Senker, Z. Naturforsch., B: Chem. Sci. 57 (2002) 1446.
[64] S.L. Heath, P.A. Jordan, I.D. Johnson, G.R. Moore, A.K. Powell, M. Helliwell, J. Inorg. Biochem. 59 (1995) 785.
[65] S.P. Petrosyants, M.A. Malyarik, A.B. Ilyukhin, Russ. J. Inorg. Chem. 40 (1995) 765.
[66] L. Spiccia, H. Stoeckli-Evans, W. Marty, R. Giovanoli, Inorg. Chem. 26 (1987) 474.
[67] J.A. Laswick, R.A. Plane, J. Am. Chem. Soc. 81 (1959) 3564.
[68] D.J. Hodgson, M.H. Zietlow, H.E. Pedersen, M.H. Toftlund, Inorg. Chim. Acta 149 (1988) 111.
[69] J.T. Veal, W.E. Hatfield, D.Y. Jeter, J.C. Hempel, D.J. Hodgson, Inorg. Chem. 12 (1973) 342.
[70] J.T. Veal, D.Y. Jeter, J.C. Hempel, R.P. Eckberg, W.E. Hatfield, D.J. Modgson, Inorg. Chem. 12 (1973) 2928.
[71] K. Michelsen, Acta Chem. Stand. Ser. A 30 (1976) 521.
[72] E. Kiss, T. Kiss, M. Jezowska-Bojczuk, J. Coord. Chem. 40 (1996) 157.
[73] A. Lakatos, I. Bányai, R. Bertani, P. Decock, T. Kiss, Eur. J. Inorg. Chem. (2001) 461.
[74] T. Kiss, P. Buglyo, D. Sanna, G. Micera, P. Decock, D. Dewaele, Inorg. Chim. Acta 239 (1995) 45.
[75] M. Matzapetakis, M. Dakanali, C.P. Raptopoulou, V. Tangoulis, A. Terzis, J. Giapintzakis, A. Salifoglou, J. Biol. Inorg. Chem. 5 (2000) 469.
[76] M. Kilyén, I. Labádi, E. Tombácz, T. Kiss, Bioinorg. Chem. Appl. 1 (2003) 321.
[77] L.V. Kochian, D.L. Jones, in: R.A. Yokel, M.S. Golub (Eds.), Research Issues in Aluminum Toxicity, Taylor & Francis, Washington, DC, 1997, p. 69.
[78] M. Menelaou, C.P. Raptopoulou, A. Terzis, V. Tangoulis, A. Salifoglou, Eur. J. Inorg. Chem. (2006) 1957.
[79] G.C. Valle, G.G. Bombi, B. Corain, M. Favarato, P. Zatta, J. Chem. Soc., Dalton Trans. (1989) 1513.
[80] T. Moseley, J.O.W. Norris, E. Williams, in: Techniques and Mechanisms in Gas Sensing, Adam Hilger Series on Sensors, I.O.P. Publishing, Bristol, 1991.

[81] S.L. Heath, A.K. Powell, H.L. Utting, M. Helliwell, J. Chem. Soc., Dalton Trans. (1992) 305.
[82] J.C. Goodwin, S.J. Teat, S.L. Heath, Angew. Chem., Int. Ed. 43 (2004) 4037.
[83] S.L. Heath, A.K. Powell, Angew. Chem., Int. Ed. Engl. 31 (1992) 191.
[84] A.K. Powell, S.L. Heath, D. Gatteschi, L. Pardi, R. Sessoli, G. Spina, F. Del Giallo, F. Pieralli, J. Am. Chem. Soc. 117 (1995) 2491.
[85] H.R. von Uexküll, E. Mutert, Plant Soil 171 (1995) 1.
[86] A. Salifoglou, Coord. Chem. Rev. 228 (2002) 297.
[87] K. Takeda, T. Yamashita, A. Takahashi, C.F. Timberlake, Phytochemistry 29 (1990) 1089.
[88] C.F. Timberlake, J. Gem. Sot. 561 (1959) 2795.
[89] A. Salifoglou, in: M. Gielen, E.R.T. Tiekink (Eds.), Metallotherapeutic Drugs & Metal-based Diagnostic Agents: The Use of Metals in Medicine, John Wiley & Sons Ltd., England, 2005, p. 65.